Applied Numerical Modeling in Geomechanics – 2020 – Billaux, Hazzard, Nelson & Schöpfer (eds.) Paper: 10-02

Paths of force chains at the cyclic threshold shear strain in sand

Vedran Pavlic & Tomislav Ivsic
University of Zagreb, Faculty of Civil Engineering, Zagreb, CROATIA

1 INTRODUCTION

Granular material (sand) subjected to cyclic loading is characterized by the change of: shear modulus, pore water pressure (PWP) and volume. The change occurs when the amplitude of the cyclic shear strain (amplitude) exceeds a certain value, the cyclic threshold shear strain (threshold). The consequences of exceeding the threshold are reflected as cyclic phenomena: settlement, PWP buildup, stiffening and degradation of strength (Barkan 1962, Drnevich & Richard 1970, Silver & Seed 1971, Dobry et al. 1982, Tabata & Vucetic 2010).

In order to explore these phenomena, it is necessary to model the force transmission in the sand depending on the amplitude. The force chains play a key role as a force transmission mechanism in the sand and determine the mechanical properties of the material: stability (forming support columns), elasticity (representing springs if there is no buckling) and flow (blocking the flow of the sand at discharge). When the load is changed, their configuration changes; they are formed, stiffened, degraded, and they disappear.

A force chain is the path through which compressive forces are transmitted in the maze of the grains and voids. The existence of force chains was discovered experimentally (Dantu 1968) using Plexiglas and Pyrex grains. A force chain consists of at least three grains that carry loads, and several force chains form a spatial network of force transmission. There are two networks of contact forces that complement each other and show a different mechanical behavior, (see e.g. Radjai et al. 1998). The weak network behaves like a fluid and the strong network like a skeleton (assumes shear stress).

Using *PFC3D* (Itasca 2014) distinct-element numerical models, along with laboratory tests on the direct simple shear (NGI-DSS) device (Bjerrum & Landva 1966), the micro-level system elements are connected with the behavior of a real sample under controlled conditions. In this way it is possible to check different hypotheses in the study of granular material. Predictable steps in the process of forming, stiffening and degrading the force chains to be modeled and monitored are shown in Table 1.

Table 1. Assumptions concerning the development of force chains during cyclic loading.

Step	Experiment	Amplitude	Description of the mechanical behavior of the force chains
1	sample formation	n/a	strong force chains build a skeleton
2	shearing	small	the number of strong network contacts gradually increases (more grains support strong force chains), the strength of the skeleton and the entire sample increases
3	shearing	medium	change of the behavior of the material, i.e. threshold
4	shearing	large	there is buckling and failure of strong force chains, the number of contacts and the strength of the sample decreases rapidly, and after a certain number of cycles, flow occurs

2 DESIGN AND ANALYSIS

Numerical analysis includes: modeling of boundary conditions, generation of synthetic material, sample preparation, selection and calibration of the contact model, test simulation, and extracting and processing a series of collected data. A more detailed description of modeling, generating and preparing the sample is given in the paper (Pavlic et al. 2017).

2.1 *Numerical modeling of NGI-DSS device*

By modeling the elements of the NGI-DSS device that enclose the sample (typical dimensions of a specimen are: height of about 19 mm and diameter of 67 mm), boundary conditions have been defined. The sample is enclosed laterally by a membrane, and by porous discs and caps on the upper and bottom sides, see Figure 1. In the numerical model, caps are modeled using walls (hollow cylinder) and porous discs are modeled as clumps (spheres arranged in the form of a honeycomb).

The membrane is a nickel alloy spiral wire coated in rubber and is in this case modeled as follows: the spiral is broken into rigid horizontal rings (clumps), the rings are aligned vertically and linked using the linear parallel-bond contact model that enables the transmission of momentum and tensile force between them.

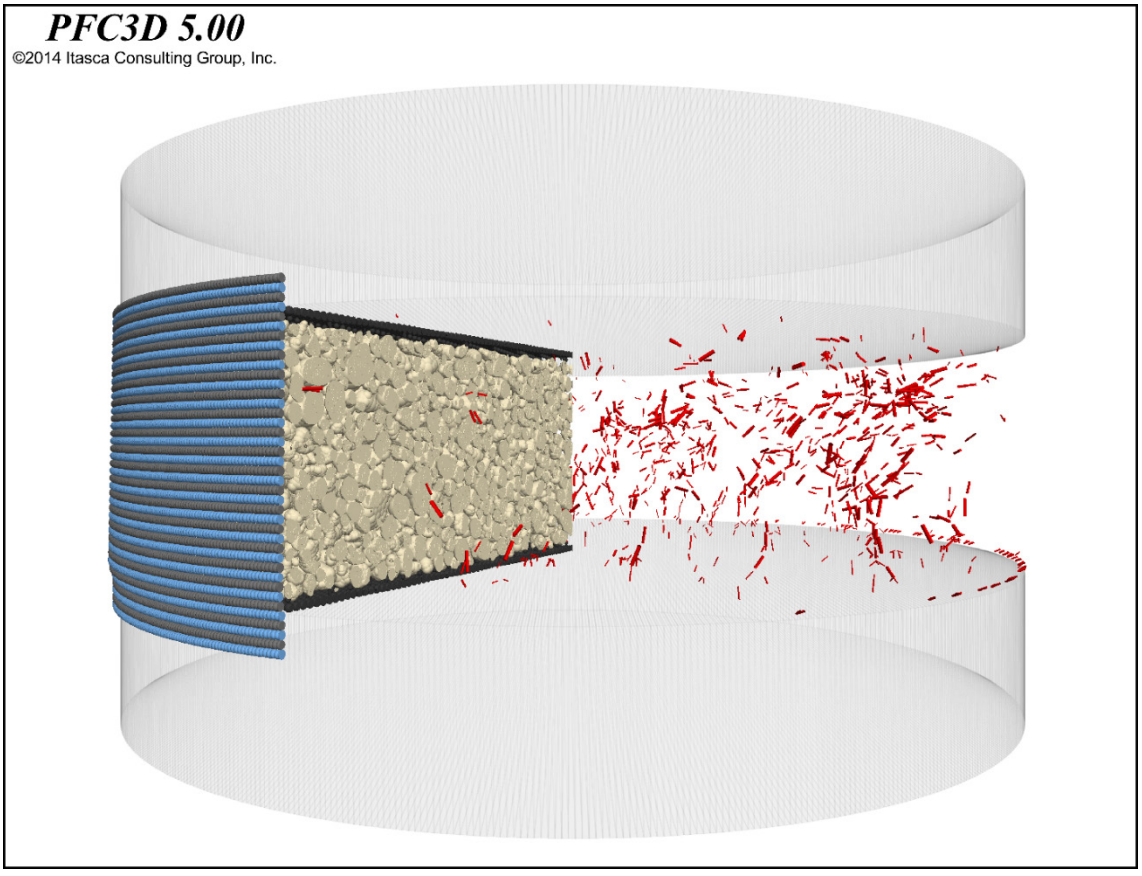

Figure 1. Model overview of the NGI-DSS device (transparent caps, black discs, blue and anthracite membrane rings), sand (model of clumps) and force chains defined by the user (red cylinders).

2.2 *Numerical modeling of sand*

Two types of sand models will be used in the research: a) A numerical model of spheres with a regular arrangement of the grains (the grains are organized centrally into columns and rows); and b) A numerical model of clumps with a random organization of the grains and irregular grain shapes (clump, 11 fractions). The importance of the sphere model is the comparison with the theoretical model and the importance of the clump model is studying the impact of the grain shape on the effects of arching and grain interlocking.

In order to determine the minimal number of grains in the model that gives realistic results, the grains are scaled (the membrane and the discs retain the actual dimensions). By comparing the shear results of the models with different magnifications (ranging from 5 to 15), the effect of magnification will be determined, and the duration of the numerical simulation will be optimized. During magnification, a real granulometric curve is retained without 6% of the smallest particles.

2.3 *Contact model selection*

In the system of solid grains, the distinct element method (Cundall 1979) takes into account each grain individually. Grain motion is determined based on the interrelation with adjacent grains using a circular calculation process. In the circular procedure, calculations on the grain contact (calculations of the contact force and moment) are interchanged with the grain motion calculation (linear and rotational motion).

Contacts are resolved using the following mechanical models: spring (stiffness component), slider (strength component) and piston (viscous damping component). The stiffness component uses the modified Hertz model (Mindlin & Deresiewicz 1953). The strength component, i.e. the yield limit, depends on the friction coefficient (Coulomb 1781) and the damping coefficient is determined by trial and error.

2.4 *NGI-DSS test simulation*

NGI-DSS test simulation consists of two stages. In the first stage, the sample is loaded vertically. In the second stage, the upper disk is maintained at the constant height and sheared at given cyclic sinusoidal strains, while the vertical boundaries of the membrane rotate for the value of the amplitude. By maintaining a constant height of the upper disc during shear, the experiment is carried out under equivalent undrained conditions, i.e. at constant volume (Taylor 1953).

The concept equates the testing of a fully saturated sample under undrained conditions (constant volume) with a dry sample without water while maintaining a constant height (constant volume). Pore water pressure is in reality zero during the test, while the change in vertical stress (in order to maintain a constant height) is equal to the change in the PWP that would develop in an actual undrained test, see (Hsu & Vucetic 2006).

2.5 *Query Results*

Force chains as a stiffer element (in relation to the rest of the material trapped between them) define the displacement, i.e. the behavior of the system. In order to define the role of the force chain, it is necessary to isolate and filter directed and large contact forces among the heap of contact forces according to the requirements of the user. Contact forces *i* and *j* are considered to be members of the same force chain in the following case:

- contact forces exceed a certain value (percentage of the maximum contact force);
- contact forces share the same clump; and
- unit vectors of contact forces close an angle of less than 30° or more than 150°.

3 RESULTS AND DISCUSSION

The *PFC3D* allows each grain (displacement, velocity, rotation), grain series (direction and magnitude of the contact forces), and average values of stress and deformations at larger volumes to be monitored. Threshold, force chain stability, change of the shear modulus and PWP are explored by monitoring the number of contacts, porosity and stress-strain relationship depending on the amplitude.

3.1 *Results on mesoscopic level*

In order to analyze the mesoscopic level results associated with the configuration of the force chains, a code that filters the contact forces according to user requirements was written, see Figure 1. When filtering contact forces with regard to their magnitude, the mean value is not applicable. In order to filter contact forces with regard to their magnitude, it is necessary to use the force distribution function, i.e. to weigh the contact forces. In the later phase of the study, the force chains whose failure represents the beginning of the shear modulus change and the PWP buildup, as well as the cause of the failure will be isolated.

3.2 *Results on macroscopic level*

The results of the NGI-DSS test, and thus the results of the test simulation on macroscopic level, are presented in the form of closed curves on the stress-strain diagram (loops). The loop represents the basic element of the dynamic behavior of the soil from which it is possible to get a shear modulus and damping (Kramer 1996). By joining the loop tips, the shear modulus reduction curve (G_N/G_{max}) is obtained relative to the amplitude (γ_c), where G_{max} is G at $\gamma_c < 1 \cdot 10^{-3}$ %. The reduction curve is also shown depending on the number of cycles (N).

Instead of the usual display of the reduction curve with the equivalent material damping curve, the damping curve is replaced by a normalized excess PWP, i.e. the relationship between the change of the PWP and the initial vertical stress ($\Delta u/\sigma_{vc}$) in relation to the amplitude, see Figure 2. From the aforementioned curve combination, it is possible to see the threshold value (for laboratory test value is $1 \cdot 10^{-2}$ %) after which the mechanical behavior of the sand is changed.

Figure 2 shows the results of the uncalibrated sphere model (grains are magnified by 15 times) and the results of the uncalibrated clump model (grains are magnified by 7 times). In both models it is possible to see a sudden change in mechanical behavior after the deformation threshold has been exceeded. In the later stage of the study, the parameters of the contact model will be calibrated based on laboratory tests.

The threshold values for cyclic phenomena range from 0.007 to 0.03%, see Table 2. It can be concluded that all four experimentally tested thresholds are very similar or identical, see (Dobry et al. 1982). The reason is the dominant physical process that applies equally to all four thresholds, and refers to the failure of force chains.

Table 2. Threshold values in sands established by laboratory tests.

Phenomenon	Threshold mark	Threshold value (%)	Source	Condition
settlement	γ_{tv}	0,007 – 0,03	Vucetic 1994	drained
stiffening	γ_{ts}	0,01	Drnevich & Richard 1970	
PWP buildup	γ_{tp}	0,01 – 0,02	Hazirbaba & Omarow 2015	undrained
degradation	γ_{td}	could not be defined	Mortezaire 2012	

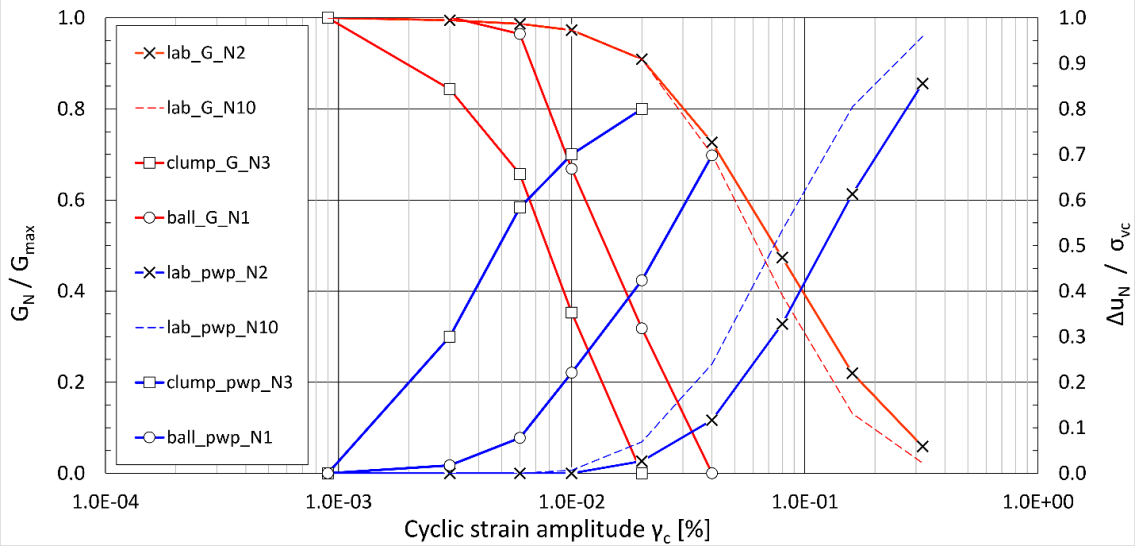

Figure 2. The change of the normalized shear modulus and the normalized excess PWP depends on the amplitude size and number of cycles for the laboratory tests, numerical model of spheres and the numerical model of clumps.

4 CONCLUSIONS

In order to obtain a complete picture of the mechanical behavior of the granular material, it is necessary to use different levels of observation. It is expected that the definition of principles on microscopic level that corresponds to the response of the granular material on a macroscopic level (numerical model makes that possible) should allow the following: determining the control mechanism of mechanical behavior of the sand before and after the threshold; determining the key factors affecting the threshold size; defining the role of the force chains; understanding dynamic phenomena, such as liquefaction, wave propagation, avalanche and earthquake, and explain the different values of the shear modulus obtained through dynamic and cyclic tests.

ACKNOWLEDGEMENT

The author Vedran Pavlic is a recipient of the Itasca Education Partnership program and the use of Itasca codes including *PFC3D*. We are grateful for their support.

REFERENCES

Barkan, D.D. 1962. Dynamics of bases and foundations. McGraw-Hill Book Company: New York.

Bjerrum, L. & Landva, A. 1966. Direct Simple Shear Tests on Norwegian Quick Clay. *Geotechnique* 16(1): 1-20.

Coulomb, C.A. 1781. Theorie des machines simple, en ayant egard au frottement de leurs parties et a la roideur des Corages. *Piece qui remporte le Prix double de l`Academie de Sciences pour l`annee 1781*.

Cundall, P.A. & Strack, O.D.L. 1979. A discrete numerical model for granular assemblies. *Geotechnique* 29(1): 47-65.

Dantu, P. 1968. Etude experimentale d`un milieu pulverulent: compris entre deux plans verticaux et paralleles. *Annales des ponts et chaussees* 4: 193-202.

Dobry, R., Ladd, R.S., Yokel, F.Y., Chung, R.M. & Powell, D. 1982. Prediction of pore water pressure buildup and liquefaction of sands during earthquakes by the cyclic strain method. *NBS BSS* 138.

Drnevich, V.P. & Richart, F.E. 1970. Dynamic prestraining of dry sand. *Journal of the soil mechanics and foundation division; Proceedings of the ASCE* 96(SM2): 453-469.

Hazirbaba, K. & Omarow, M. 2015. Post-cyclic loading settlement of saturated clean sand. *Soil Dynamics and Earthquake Engineering.* (77): 337–347.

Hsu, C.C. & Vucetic, M. 2006. Threshold Shear Strain for Cyclic Pore-Water Pressure in Cohesive Soils. *Journal of geotechnical and geoenviromental engineering; ASCE* 1325-1335.

Itasca Consulting Group, Inc. 2014. *PFC3D – Particle Flow Code in 3 Dimensions, Ver. 5.0 User's Manual.* Minneapolis: Itasca.

Kramer, S.L. 1996. Geotechnical Earthquake Engineering. Prentice Hall

Mindlin, R.D. & Deresiewicz, H. 1953. Elastic Spheres in Contact under Varying Oblique Force. *Trans. ASME, J. Appl. Mech.* 20: 327-344.

Mortezaie, A.R. 2012. Cyclic threshold strains in clays versus sands and the change of secant shear modulus and pore water pressure at small cyclic strains. Ph.D. thesis, University of California, Los Angeles.

Pavlic, V., Matesic L. & Kvasnicka, P. 2017. Numerical modelling of the NGI-DSS test and cyclic threshold shear strain for degradation in sand. *Granular Matter* (19): 37.

Radjai, F., Wolf, D.E. & Moreau, J.J. 1998. Bimodal Character of Stress Transmission in Granular Packings. *Physical review letters* 80(1): 61-64.

Silver, M.L. & Seed, H.B. 1971. Volume Changes in Sands During Cyclic Loading. *Journal of the Soil Mechanics and Foundations Division; Proc. ASCE* 97(SM9): 1171-1182.

Tabata, K. & Vucetic, M. 2010. Threshold shear strain for cyclic degradation of three clays. *Fifth International Conference on Recent Advances in Geotechnical Earthquake Engineering and Soil Dynamics and Symposium in Honor of Professor I.M. Idriss*. San Diego.

Taylor, D.W. 1953. A direct shear test with drainage control. *Symposium on Direct Shear Testing of Soils, edited by G. Tschebotarioff. ASTM* (STP) 131: 63-74.

Vucetic, M. 1994. Cyclic Threshold Shear Strains in Soils. *Journal of Geotechnical Engineering. ASCE* 120: 2208-2228.